www.ptcer.pl/mccm

MATERIAŁY CERAMICZNE /CERAMIC MATERIALS/, 63, 1, (2011), 157-163

# Impedance Spectroscopy Study of Electrode-Electrolyte System in Solid Oxide Fuel Cells

**Mariusz Krauz[1], Marta Radecka[2], Mieczysław Rękas[2]***

[1] Institute of Power Engineering, Ceramic Department CEREL, ul. Techniczna 1, 36-040 Boguchwała, Poland
[2] AGH University of Science and Technology, Faculty of Materials Science and Ceramics
al. Mickiewicza 30, 30-059 Kraków, Poland
*e-mail: rekas@agh.edu.pl

***Abstract***

Planar electrolyte-supported solid oxide fuel cells were studied. Dense membranes of the dimensions: 100 x 100 mm and a thickness of 130 μm, made from yttria-stabilized zirconia (both tetragonal and cubic) were used as solid electrolytes. Ni-zirconia cermet and $La_{0.8}Sr_{0.2}MnO_3$ layers were deposited on the surfaces of the electrolyte as the anode and the cathode, respectively. Electrochemical impedance spectroscopy was used in order to characterize the electrical properties of the solid electrolyte membranes and the electrolyte-anode and electrolyte-cathode systems. It was found that an equivalent circuit is composed of two series of resistor- constant phase element connected in parallel. No additional elements in the equivalent circuit originated from either the anode or the cathode layers have been observed with respect to the single electrolyte sample.

**Keywords:** SOFC, YSZ, Anode-cermet zirconia-Ni, Cathode - $La_{0.8}Sr_{0.2}MnO_3$

**BADANIA SPEKTROSKOPII IMPEDANCYJNEJ UKŁADU ELEKTRODA-ELEKTROLIT W STAŁOTLENKOWYCH OGNIWACH PALIWOWYCH**

Zbadano płaskie stałotlenkowe ogniwa paliwowe osadzone na elektrolicie. Jako elektrolit stały wykorzystano gęste membrany o wymiarach 100 x 100 mm i grubości 130 μm, wykonane z dwutlenku cyrkonu stabilizowanego tlenkiem itru, zarówno tetragonalnego jaki i regularnego. Cermet Ni-$ZrO_2$ i warstwy $La_{0.8}Sr_{0.2}MnO_3$ osadzano na powierzchniach elektrolitu, odpowiednio jako anodę i katodę. Wykorzystano elektrochemiczną spektroskopię impedancyjną, aby scharakteryzować właściwości elektryczne membran elektrolitu stałego i układów elektrolit-anoda i elektrolit-katoda. Stwierdzono, że obwód równoważny zbudowany jest z dwóch serii elementów rezystor-faza stała, połączonych równolegle. W odniesieniu do próbki pojedynczego elektrolitu nie zaobserwowano żadnych dodatkowych elementów obwodu równoważnego pochodzących od warstw anody ani katody.

**Słowa kluczowe:** SOFC, YSZ, anoda-cermet $ZrO_2$-Ni, katoda - $La_{0.8}Sr_{0.2}MnO_3$

## 1. Introduction

The current efforts in the research and development of solid oxide fuel cells are focused on cutting its manufacturing and maintenance costs by reducing the operating temperatures to 800°C or less [1]. One of the problems associated with lowering the operating temperature is an increase in the ohmic loss of the electrolyte and polarization losses at both electrodes. Zirconia electrolytes such as yttria-stabilized zirconia, YSZ, have been commonly used in the construction of high performance solid oxide fuel cells, SOFCs, due to the high stability they offer [2-5]. Their ohmic losses can be reduced by decreasing the electrolyte thickness. On the other hand, the polarization losses can be reduced by improving the electrochemical activity of both electrodes [6, 7]. Taking into account the fact that electrode reactions occur on the triple-phase boundary (TPB) involving a gas phase, and ionic and electronic conductors, making the optimal choice of both the chemical composition of the electrodes and their microstructures is a challenging task. Two main techniques have been used to study solid-state electrochemical systems: dc polarization measurements [8] and electrochemical impedance spectroscopy, EIS [8, 9]. Especially EIS is an important research tool for studying the bulk properties, and the interface and electrode electrochemical reactions [1]. In particular, it may be useful for testing the materials used in solid oxide fuel cells, SOFCs [2]. The proper determination of the influence of different components on the overall internal electrical resistivity of the fuel cell makes it possible to optimize cell performance. The aim of this work was to study the afore-mentioned solid electrolytes (both tetragonal and cubic yttria-doped zirconia), as well as the electrolyte-electrode system (either cathode or anode of the SOFC), by means of the EIS method.

## 2. Experimental

High purity YSZ powders provided by Tosoh Corporation, Tokyo, Japan, containing either 3 mol.% $Y_2O_3$ (tetragonal form) or 8 mol.% $Y_2O_3$ (cubic form) (TZ-3Y and TZ-8Y, re-

spectively) were used as starting materials, to prepare the membranes used as the solid electrolytes. They are referred to as 3YSZ and 8YSZ further on. The powders were mixed with a binder (PVB, Ferro) to form slurries which were used to form ceramic foil casting. The foils were dried and thermally treated at 1500°C for 1 h. The dimensions and thickness of the foils after sintering were 10 x 10 cm and between 80 and 150 μm, respectively. They were used in electrical measurements and in the formation electrode-electrolyte systems. Electrodes were deposited on one surface of the foil using the screen-printing method. $La_{0.8}Sr_{0.2}MnO_3$ (LSM) and the electrolyte-Ni (1:1) composite were used as the cathode and the anode of the fuel cell, respectively. Silver measuring electrodes were then deposited on both surfaces of the specimens. The impedance measurements were performed using a frequency response analyzer (Solartron, model FRA 1260) coupled with a dielectric interface (Solartron, model 1296). The frequency range was 10 mHz - 1 MHz, and the amplitude of the sinusoidal voltage was 10 mV. The measurements were done in the temperature range 428-1030 K. The gas atmosphere during measurements was flowing synthetic air in the case of electrolytes and electrolyte-cathode systems. On the other hand, a flowing Ar+8 % $H_2$ gas mixture was used in the case of electrolyte-anode systems. The measurements were done in typical sample holder, which allowed the control of temperature and gas atmosphere composition. The resistances of both grain interior, $R_b$, and grain-boundary, $R_{gb}$, were determined by fitting the complex impedance data using the equivalent circuit resulting from the brick-wall model [5, 6]. The ZPLOT software package provided by Solartron was used for this purpose. The electrical conductivity was calculated from the formula:

$$\sigma = \frac{d}{S \cdot R} \tag{1}$$

where σ – electrical conductivity, $d$ – sample thickness and $S$ – electrode surface area.

Both grain interior, $\sigma_b$, and grain boundary, $\sigma_{gb}$, conductivity was determined. However, it should be mentioned that the $\sigma_{gb}$ value obtained in this way is only an apparent one. The real grain boundary conductivity may be determined if the exact grain boundary coverage fraction of the studied sample is known [10].

## 3. Results and discussion

Fig. 1 shows SEM photographs of the electrolyte-electrode systems. The cross-section of the LSM cathode (left side) / 3YSZ electrolyte (right side) structure is presented in Fig. 1a. The electrolyte layer is uniformly continuous, pore-free and adheres well to the cathode layer. On the other hand, the cathode layer is formed of uniform grains with randomly distributed pores. The microstructures of the 3YSZ and 8YSZ systems with cermet anode layers are presented in Figs. 1b and 1c, respectively.

Both electrolytes are composed of grains with different sizes and shapes. In this case, the electrolyte and anode layer also adhere well. Figs. 2 and 3 show the typical impedance spectra for 3YSZ and 8YSZ, respectively, as measured at several temperatures between 428-813 K.

Below 695 K, two well-defined semicircles are visible, one at high and the other at lower frequencies. Above this

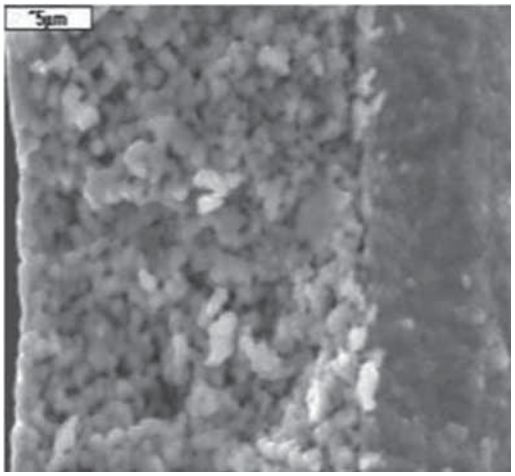


a)

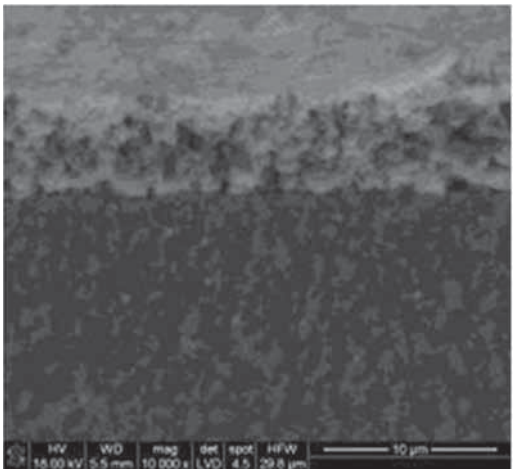


b)

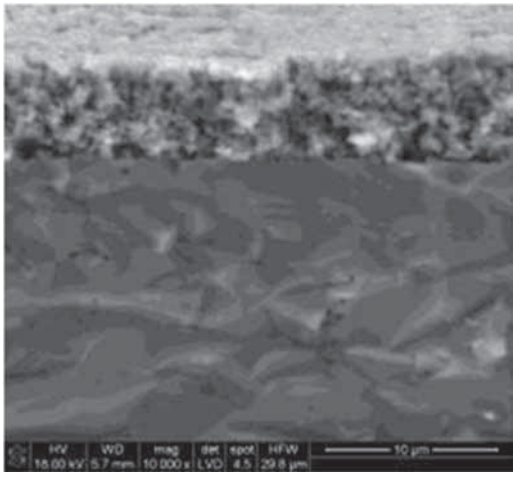


c)

*Fig. 1. SEM images of the electrolyte/electrode systems: a) LSM-cathode (left side) / 3YSZ-electrolyte (right side) cross-section, b) Ni-YSZ cermet-anode (top) / 3YSZ (bottom), c) Ni-YSZ cermet-anode (top) / 8YSZ (bottom).*

temperature, only one semicircle can be distinguished. A careful analysis of the impedance spectra revealed that the centre of the semicircles is placed below the Z' axis, which indicates that constant phase elements, CPEs, should be selected for the equivalent circuit instead of Debye capacitors. The equivalent circuits used for fitting the experimental data consisted of either $\{R_b\text{-}CPE_b\}$–$\{R_{gb}CPE_{gb}\}$ (Fig. 4a) or $R_b$–$\{R_{gb}CPE_{gb}\}$ (Fig. 4b) elements. According to well docu-

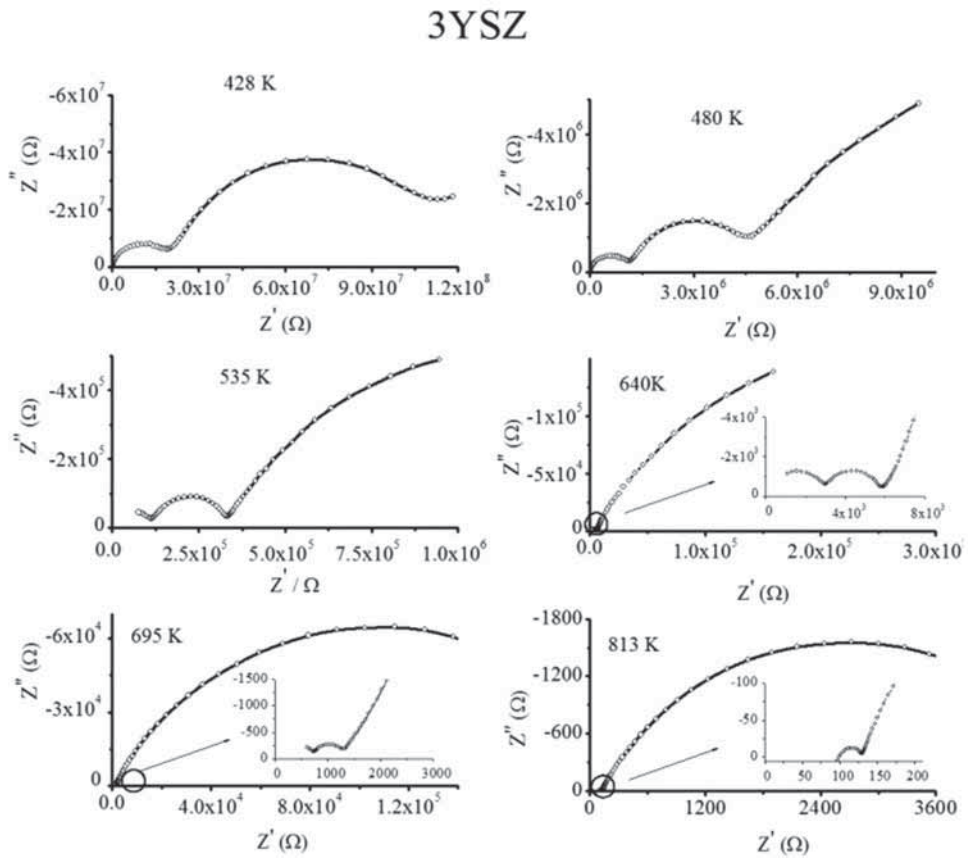


*Fig. 2. Impedance spectra for 3YSZ as a function of temperature.*

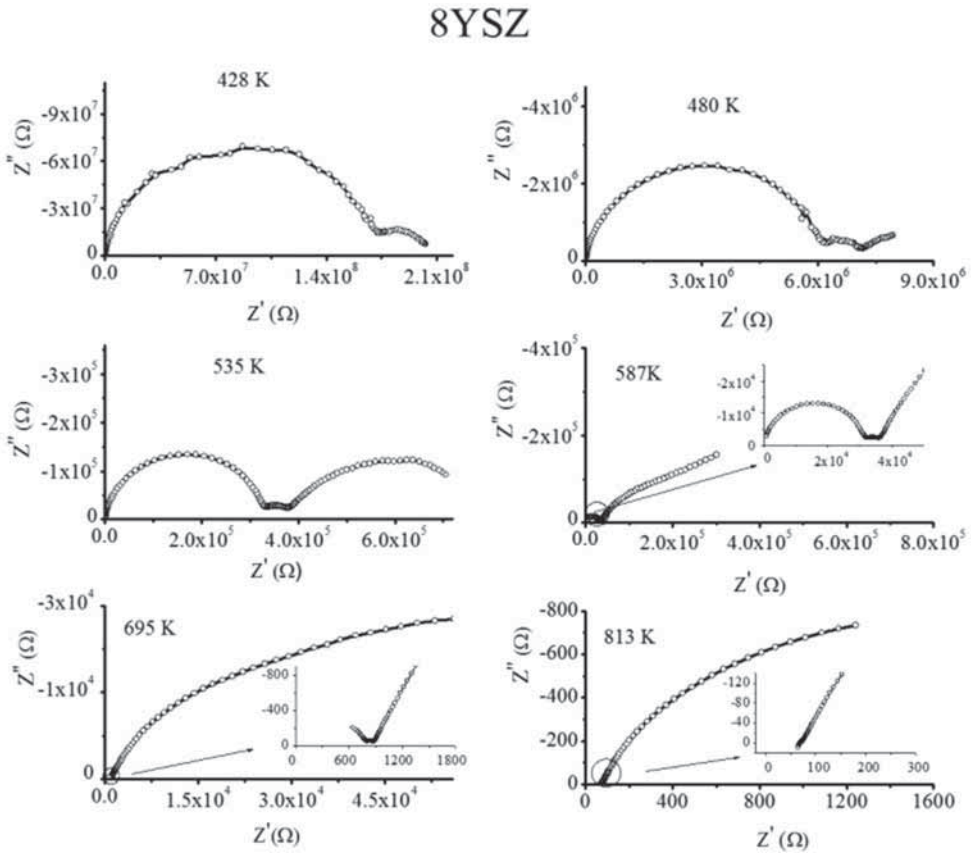


*Fig. 3. Impedance spectra for 8YSZ as a function of temperature.*

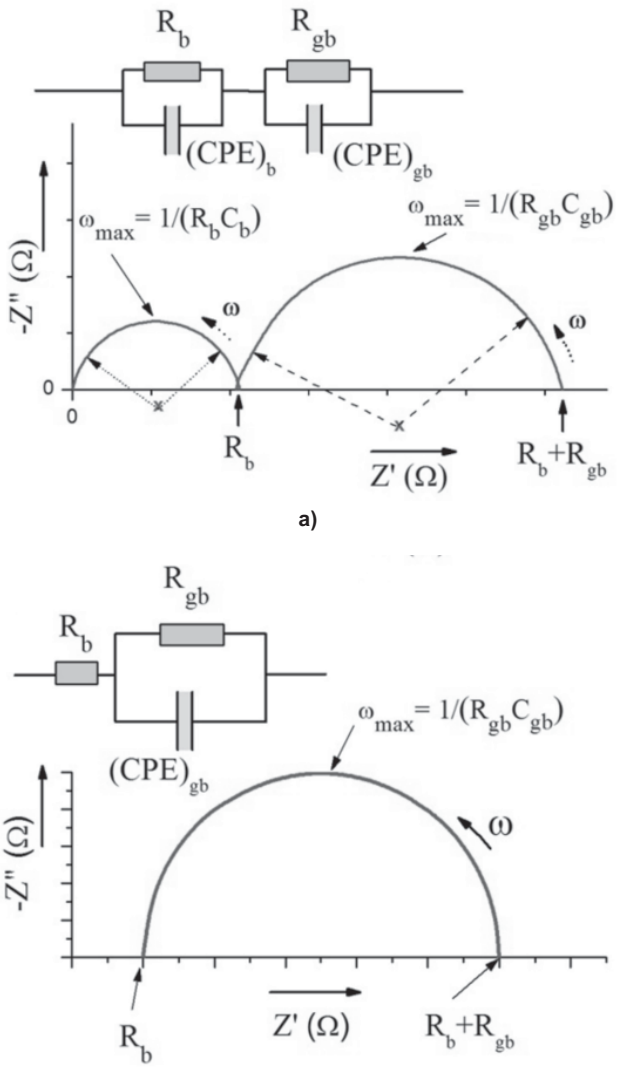


*Fig. 4. Equivalent circuits and corresponding impedance spectra: a) at lower temperatures (below 695 K), b) at higher temperatures (above 695 K).*

mented studies, the higher-frequency part of the spectrum can be attributed to bulk properties, and the lower-frequency part is related to grain boundary properties [11].

Representative impedance spectra of the electrolyte-electrode systems, measured at 480 K, are shown in Figs. 5 and 6. The presented spectra are similar to that of a single electrolyte, shown in Figs. 2 and 3. No additional arcs resulting from the electrode layers were observed.

The impedance of the CPE components, $Z_{CPE}$, in the equivalent circuits (Fig. 4) can be expressed as:

$$Z_{CPE} = \frac{1}{A \cdot (j \cdot \omega)^n} \qquad (2)$$

where $A$, $n$ – constants, $j$ – imaginary unit, $\omega$ – angular frequency.

Fig. 7 illustrates the temperature dependencies of the exponents $n_1$ and $n_2$ that describe the elements of $CPE_b$ and $CPE_{gb}$, respectively. The presented parameters differ substantially from those predicted for Debye elements: capacitor ($n = 1$), resistor ($n = 0$), as well as Warburg impedance ($n = 0.5$) [9]. This happens very often in oxide systems. In general, the *CPEs* are associated with material inhomogene-

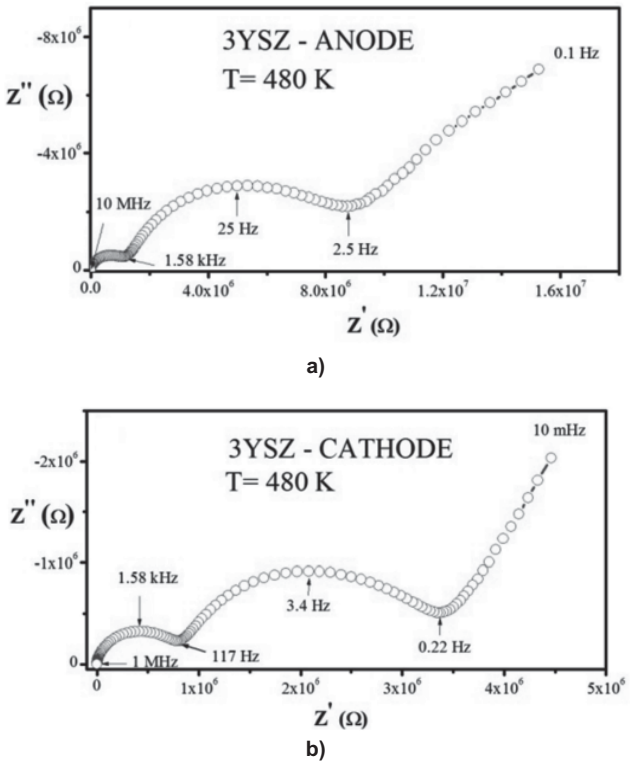


*Fig. 5. Impedance spectra at 480 K for: a) 3YSZ/anode, b) 3YSZ/cathode.*

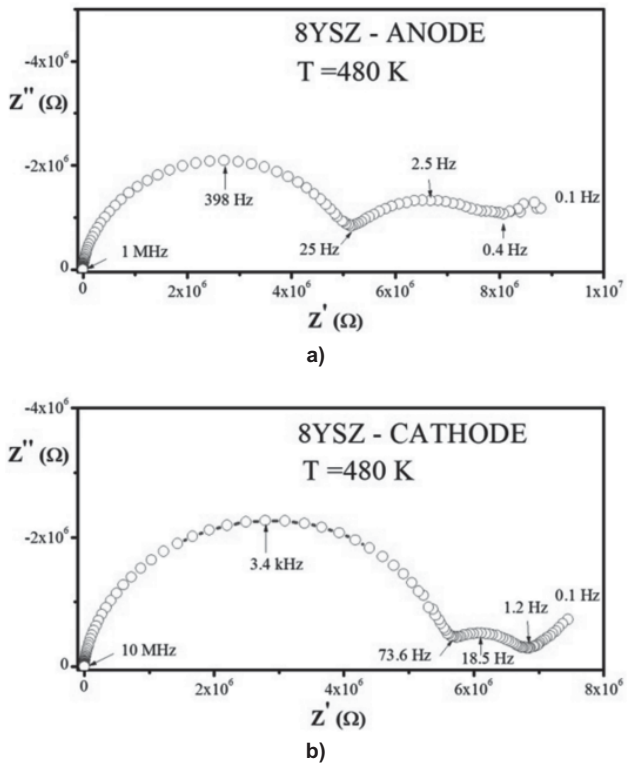


*Fig. 6. Impedance spectra at 480 K for: a) 8YSZ-anode, b) 8YSZ-cathode.*

ity, electrode roughness or porosity, and with ionic transport deviations from Fick's law [12].

Using Eq. (1), the electrical conductivities of the bulk, $\sigma_b$, and grain boundaries, $\sigma_{gb}$, were determined. The temperature dependence of both $\sigma_b$ and $\sigma_{gb}$ were fitted using the following theoretical (Arrhenius) equation:

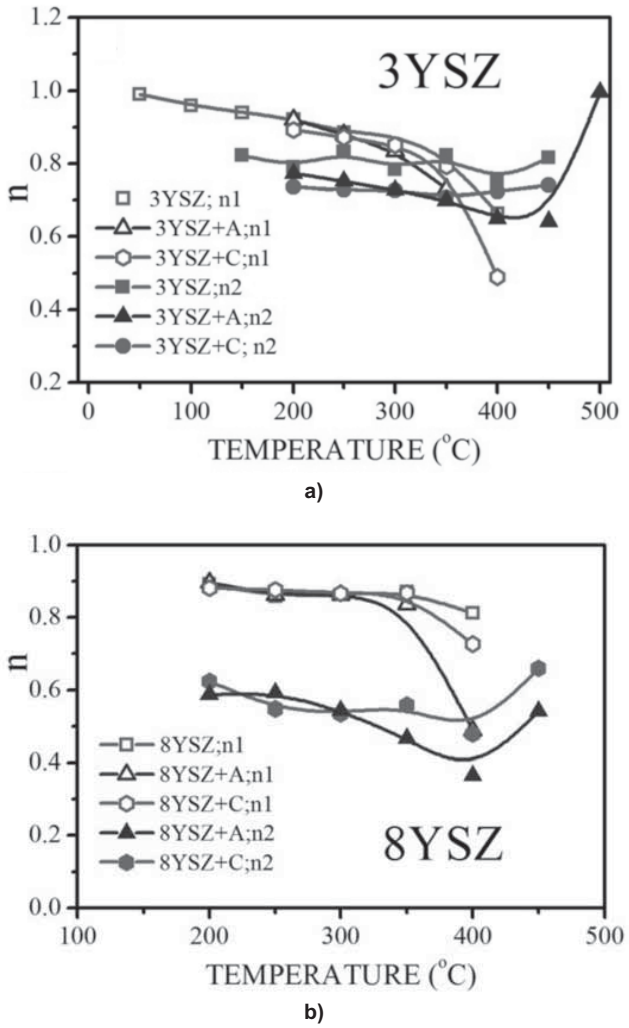


*Fig. 7. Temperature dependence of CPE parameters n of the specimens: a) 3YSZ/electrolyte (curve 3YSZ), 3YSZ/Ni-YSZ cermet-anode (curve 3YSZ+A); 3YSZ/ LSM – cathode (curve 3YSZ+C); b) 8YSZ/electrolyte (curve 8YSZ); 8YSZ/ Ni-YSZ cermet anode (curve 8YSZ+A); 8YSZ/ LSM – cathode (curve 8YSZ+C). Empty and solid markers correspond to bulk and grain boundary elements, respectively.*

$$\sigma \cdot T = A \cdot exp\left(-\frac{E}{k \cdot T}\right) \qquad (3)$$

where $T$ – temperature, $k$ – Boltzmann constant, $E$ – activation energy and $A$ – pre-exponential term, practically independent of temperature.

Figs. 8 and 9 illustrate sample dependencies of $\log(\sigma_b \cdot T)$ and $\log(\sigma_{gb} \cdot T)$ vs. $T^{-1}$ for 3YSZ and 8YSZ, respectively.

Below 650 K, electrical resistivity of grain boundaries assumes higher values than those of the bulk in 3YSZ. The activation energies, $E_b$ and $E_{gb}$, determined from the slopes of straight lines, and the parameters $\log(\sigma_b \cdot T)_0$ and $\log(\sigma_{gb} \cdot T)_0$ as intercepts of the straight lines in Fig. 8 and 9, are presented in Table 1. As can be seen from Table 1, there are no significant differences between the obtained values of activation energies and those reported for yttria-stabilized zirconia by other authors [13-23]. It is worth to mention that the activation energies and pre-exponential terms determined for electrolyte-electrode systems are very similar to those determined for single electrolyte specimens.

Figs. 10 and 11 show Arrhenius plots collected for 3YSZ and 8YSZ, respectively. There are no significant quantitative differences between electrolyte layer and electrolyte/electrode system in the case of 3YSZ (Figs. 10a and 10b). 3YSZ with the cathode layer exhibits slightly higher conductivity than the single electrolyte. On the other hand, the 3YSZ/anode system has the same bulk conductivity as 3YSZ (Fig. 10a) and lower grain boundary conductivity (Fig. 10b). The observed differences between 8YSZ and the 8YSZ/electrode system are much larger (Fig. 11). Bulk electrical conductivities of 8YSZ with either the anode or the cathode are practically equal. Above 700 K, they are slightly higher than that of the pure 8YSZ electrolyte, and below 700 K they are slightly lower.

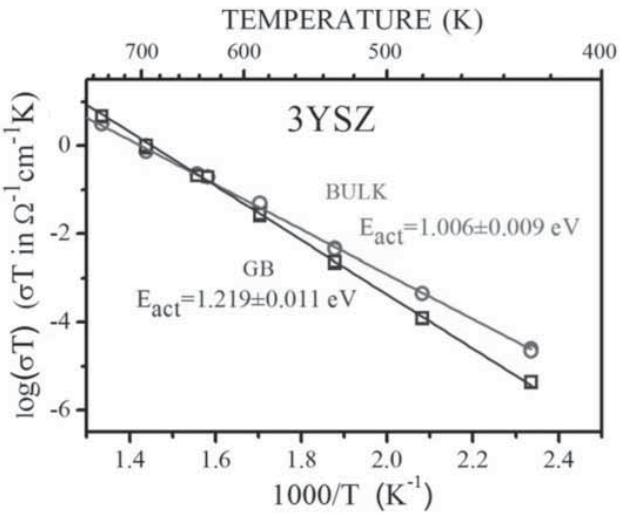


*Fig. 8. Arrhenius plot of (s·T) for 3YSZ.*

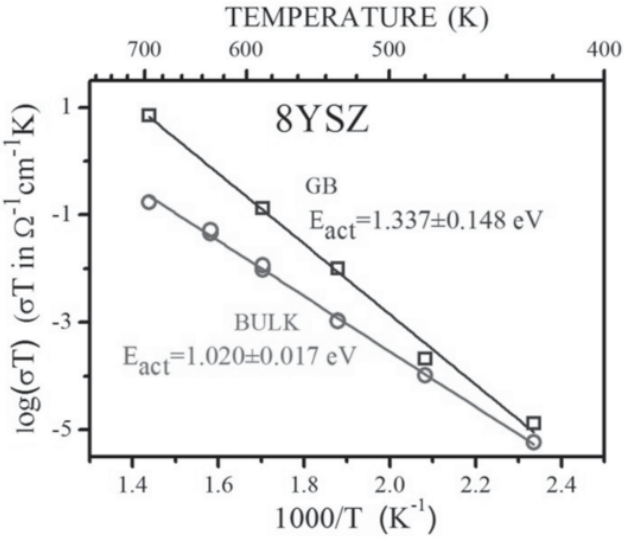


*Fig. 9. Arrhenius plot of (s·T) for 8YSZ.*

An improvement of grain boundary conductivity of 8YSZ/electrode with respect to the pure 8YSZ is observed (Fig. 11b).

The log $A$ and $E$ parameters from Eq. (2) are linearly correlated for ionic conductors [24, 25]. This correlation has been named as the compensation effect or the Meyer-Neldel rule [26], and it is valid for series of samples with similar composition.

Fig. 12 illustrates the logarithm of the pre-exponential factor, $A$, versus activation energy, $E$, for all studied specimens. Although the specimens differ considerably in their

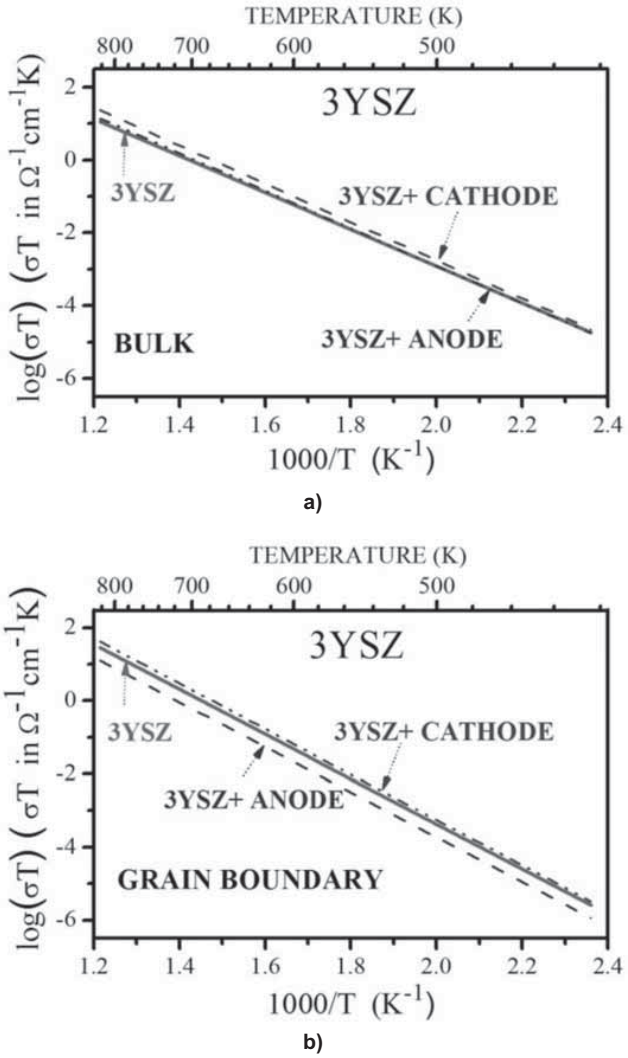


*Fig. 10. Arrhenius plots collected for 3YSZ, 3YSZ/anode and 3YSZ/cathode: a) bulk conductivity, b) grain boundary conductivity.*

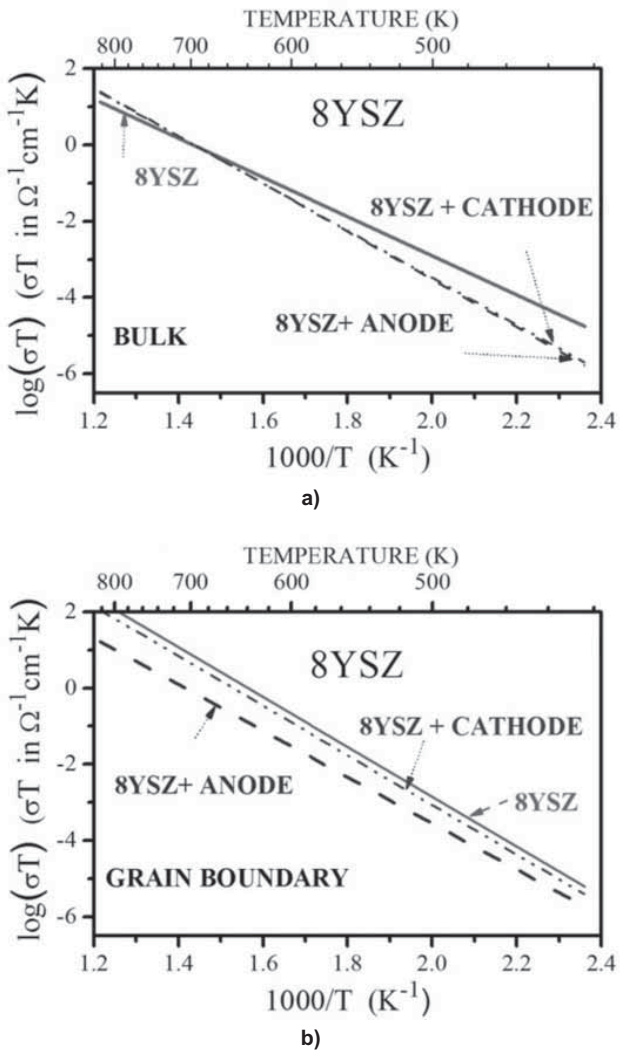


*Fig. 11. Cumulated Arrhenius plots for 8YSZ, 8YSZ/anode and 8YSZ/cathode: a) bulk conductivity, b) grain boundary conductivity.*

structure and chemical composition, all experimental data (log*A*, *E*) are in accordance with the Meyer-Neldel rule. This leads to the conclusion that the differences in the chemical composition of the investigated electrolytes and the type of used electrodes are not significant as far as the Meyer-Neldel rule is concerned.

## 4. Conclusions

Dense solid electrolyte membranes of the dimensions 100 x 100 mm and the thickness 80-150 μm, composed of either tetragonal or cubic yttria-doped zirconia, were produced by means of the foil casting method. Electrochemical impedance spectroscopy was used to determine the electrical properties of the solid electrolytes: $ZrO_2$ + 3 mol.% $Y_2O_3$ and $ZrO_2$ + 8 mol.% $Y_2O_3$. In addition, this method was also used to investigate systems composed of the solid electrolyte-anode (cermet zirconia-Ni) and the solid electrolyte-cathode ($La_{0.8}Sr_{0.2}MnO_3$). No additional arcs resulting from the electrode layers were observed. The determined activation energies of the bulk and grain boundaries conductivity were in agreement with the literature data. Furthermore, the activation energies and the pre-exponential terms obey the Meyer-Neldel rule.

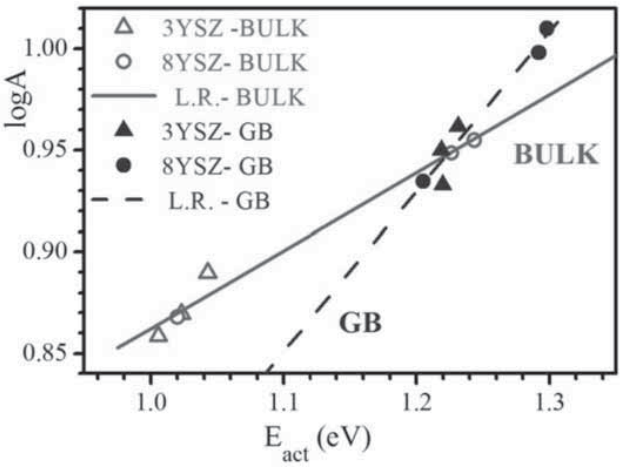


*Fig. 12. Pre-exponential factor A as a function of activation energy, E, for all studied specimens.*

## Acknowledgements

The financial support of Polish Ministry of Science and Higher Education, Project no. R15 019 02 is gratefully acknowledged.

## References


[1] Singhal S.C.: Solid State Ionics, 152-153, (2002), 405-410.
[2] Minh N.Q.: J. Am. Ceram. Soc., 76, (1993), 563-588.
[3] Sammes N.M., Du Y., Bove R.: J. Power Sour., 145, (2005), 428-434.
[4] Badwal S.P.S.: Solid State Ionics, 76, (1995), 67-80.
[5] Fuel Cell Handbook (Seventh Edition), U.S. Department of Energy, Office of Fossil Energy, Morgantown, West Virginia 26507-0880, (2004).
[6] Haile S.M.: Acta Mater., 51, (2003), 5981-6000.
[7] de Souza S., Visco S.J., De Jonghe, J.C.: J. Electrochem. Soc., 144, (1997), L35-L37.
[8] Bard A.J., Faulkner L.R.: Electrochemical Methods, Fundamentals and Applications, Wiley, New York, (1980).
[9] Barsoukov E., MacDonald J.R. (Eds.): Impedance Spectroscopy Theory, Experiment, and Applications, EDS, Willey-Interscience Publications, 2005.
[10] Zhang T.S., Ma J., Chen Y.Z., Luo L.H., Kong L.B., Chan S.H.: Solid State Ionics, 177, (2006), 1227-1235.
[11] Bauerle J.E: J. Phys. Chem. Solids, 30, (1969), 2657-2670.
[12] MacDonald J.R. (Ed.): Impedance Spectroscopy - Theory Experiment and Applications, John Wiley&Sons, New York, (1987).
[13] Verkerk M.J., Middelhuis B.J., Burggraaf A.J.: Solid State Ionics, 6, (1982), 159-170.
[14] Pimenov A., Ullrich J., Lunkenheimer P., Loidl A., Rüscher C.H.: Solid State Ionics, 109, (1998), 111-118.
[15] Cheikh A., Madani A., Touati A., Boussetta H., Monty C.: J. Eur. Ceram. Soc., 21, (2001), 1837-841.
[16] Ramamoorthy R., Sundararaman D., Ramasamy S.: Solid State Ionics, 123, (1999), 271-278.
[17] Mondal P., Klein A., Jaegermann W., Hahn H.: Solid State Ionics, 118, (1999), 331-339.
[18] Baumard J.F., Abelard P.: in Science and Technology of Zirconia II, Advances in Ceramics vol. 12, M. Rühle, A.H. Heuer (Eds.), Am. Ceram. Soc. Inc, Columbus, 1984, 555-571.
[19] Badwal S.P.S., Ciacchi F.T., Rejendran S., Drennan: J. Solid State Ionics, 109, (1998), 167-186.
[20] Petot C., Filal M., Rizea A.D., Westmacott J.Y., Laval K.H., Lacour C., Ollitrault R.: J. Eur. Ceram. Soc., 18, (1998), 1419-1428.
[21] Vitins A.: J. Solid State Electrochem., 5, (2001), 479-486.
[22] Martin M.C., Mecartney M.L.: Solid State Ionics, 161, (2003), 67-79.
[23] Wierzbicka M., Pasierb P., Rękas, M.: Physica B 387, (2007), 302-312.
[24] Almond D.P., West A.R.: Solid State Ionics, 18-19, (1986), 1105.
[25] Abtew T.A., Zhang M.L, Pan Y., Drabold D.A: J. Non-Cryst. Solids, 354 ,(2008), 2909-2913.
[26] Meyer W., Neldel H.: Z. Tech. Phys., 18, (1937), 588.


♦

*Received 1 March 2010; accepted 8 May 2010*